



Modification and characterization of solid waste: an effective adsorbent for heavy metal removal

Kumaran Chithra*, Kumar Dhivya

Department of Chemical Engineering, A.C. Tech Campus, Anna University, Chennai 600 025, India, Tel. +91-44-2235-9189; email: kchithra@annauniv.edu (K. Chithra), dhivyasrm09@gmail.com (K. Dhivya)

Received 11 May 2016; Accepted 25 November 2016

ABSTRACT

In this study, hydrothermal modification of fly ash (FA) using titanium dioxide (TiO₂) and its application as an adsorbent for the removal of Ni(II) and Zn(II) ions from aqueous solution was explored. The FA and modified FA were characterized using scanning electron microscopy, Fourier transform infrared spectroscopy and X-ray diffraction. Experiments were carried out in a batch mode to study the effect of various parameters on adsorption. The adsorption equilibrium was attained at 180 min with an optimum pH 6 for both metal ions. The kinetic study reveals that the adsorption follows pseudo-second-order model. Experimental data of adsorption have been fitted with the Langmuir, Freundlich, Dubinin–Radushkevich and Temkin equations. In order to determine the best fit isotherm, five error analysis methods were used, namely the sum-of-squared errors, the hybrid fractional error function, the Marquardt's percent standard deviation, the average relative error and the sum of absolute error. The error values demonstrated that the Freundlich isotherm model provided the best fit to the experimental data. The adsorption capacities are 4.397 and 6.226 mg g⁻¹ for Zn(II) and Ni(II) ions, respectively. The thermodynamic parameters evaluated showed that the adsorption process is spontaneous and exothermic.

Keywords: Modified fly ash; TiO₂; Adsorption process; Kinetic studies; Zn(II) and Ni(II) ions; Isotherm models

1. Introduction

Industrialization leads to the presence of heavy metals in the environment which has become a serious threat to living organisms due to its toxic effects. Heavy metals like zinc, nickel, chromium, lead, cadmium, mercury are considered as hazardous pollutants. Zinc and nickel are of great interest because of its toxicity and widespread presence in industrial sectors like electroplating, metal finishing, paint, pigments, plastics manufacturing, textiles and fertilizers [1–3]. If effluent from these industries is left untreated into water bodies, they may cause harm to human beings and environment. Long-time exposure to these waste leads to cancer, anaemia, vomiting, brain damage, etc. [4,5]. So it becomes important

to reduce the concentration of these metal ions to the permissible limits 5 and 0.02 mg L⁻¹ for Zn(II) and Ni(II) ions, respectively, prescribed by the US Environmental Protection Agency before being discharged [6].

Hence, the removal of these heavy metals from wastewater is important and several methods like adsorption, coagulation, reverse osmosis, flocculation, biological process, precipitation, ionizing and photocatalysis are used. However, many of these methods are expensive and requires large amount of water for treatment. Hence, adsorption techniques are preferred because of their advantages like low cost, ease of operation, efficiency and simplicity of the equipment. It has been reported recently that fly ash (FA) acts as an efficient adsorbent for the removal

* Corresponding author.

of heavy metals and dyes [7–11]. Very few works on heavy metal removal have been reported. Hence, this study was aimed to synthesize modified fly ash (MFA) using TiO_2 and to explore its application in the removal of Zn(II) and Ni(II) ions from wastewater.

2. Materials and methods

2.1. Preparation of the adsorbent

The characteristics of FA obtained from M/s. North Chennai Thermal Power plant (NCTP), Chennai, are shown in Table 1. This FA comes under type F as its sum of oxide (SiO_2 [57.6%], Al_2O_3 [28.5%] and Fe_2O_3 [6.6%]) is over 70% as per ASTM (American Society for Testing and Materials) standard. The pH and conductivity of FA are 10.2 and 1710 mS^{-1} respectively. The FA was washed with distilled water to remove soluble compounds like MgO , K_2O , Na_2O , etc. present in FA and then dried at 105°C – 120°C over night before modifying using TiO_2 .

Modification of FA was done as reported in [12]. FA was mixed with 2 N NaOH solution and titanium dioxide in 1,000 mL volumetric flask in a reflux condenser with constant stirring (300 rpm) for 24 h at atmospheric pressure and 100°C . The colloidal suspension was vacuum filtered, washed repeatedly using ultrapure water and dried at 115°C – 125°C . Both modified and unmodified FA were characterised using X-ray diffraction (XRD; Bruker, D8 Discover Diffractometer, USA), scanning electron microscopy (SEM; Carl-Zeiss SMT, Germany) and Fourier transform infrared (FTIR; Jasco, FT/IR-6300, USA).

2.2. Wastewater preparation

Stock solution containing ($1,000 \text{ mg L}^{-1}$) of Zn(II) and Ni(II) were prepared by dissolving 4.382 g of $\text{ZnSO}_4 \cdot 7\text{H}_2\text{O}$ and 4.488 g of $\text{NiSO}_4 \cdot 6\text{H}_2\text{O}$ using distilled water. The working solution was prepared by diluting stock solution. The pH of the metal ion solutions were adjusted to a desired value using sodium hydroxide (NaOH) and nitric acid (HNO_3). All the chemicals used are of analytical grade (Ranbaxy Fine Chemicals Ltd., India).

2.3. Batch adsorption studies

The removal of heavy metals using MFA as an adsorbent was done in a batch reactor. A series of Erlenmeyer flasks of 250 mL capacity containing desired amount of metal ion solutions of known concentrations and MFA were agitated in shaker (Orbital, Scigenics, India) at 150 rpm. The effect of time (0–210 min), initial metal ion concentration (10 – 40 mg L^{-1}), solution pH (4.0–8.0) and adsorbent dosage (2 – 14 g L^{-1}) on adsorption of Zn(II) and Ni(II) were studied.

Table 1
Characteristics of fly ash

SiO_2	57.60%
Al_2O_3	28.5%
Fe_2O_3	6.6%
Ca	1.5%
Mg	0.5%

Metal solutions with a desired dosage of the MFA were agitated in an orbital shaker (Orbital, Scigenics, India) at 150 rpm. Samples were taken at definite intervals (0–240 min) centrifuged and concentration was analysed using atomic absorption spectroscopy (Varian Spectra AA 55, USA) at 213.9 nm for Zn(II) and 236 nm for Ni(II) periodically.

Using the following equation the amount of metal ions adsorbed at any time t was calculated:

$$q_e = \frac{(C_0 - C_e)V}{m} \quad (1)$$

where q_e is the adsorption capacity of metal ions (mg g^{-1}), V is the volume of adsorbate (L), m is the amount of MFA (g), C_0 and C_e are the initial and final concentration of metal ion (mg L^{-1}), respectively.

3. Results and discussion

3.1. Characterization of adsorbent

3.1.1. Fourier transform infrared spectroscopy

The FTIR spectra of FA and MFA are shown in Fig. 1. From the spectrum of FA, the absorption peak at 3,488, 3,699, and $3,881 \text{ cm}^{-1}$ are attributed to the stretching of inner surface and inner hydroxyl groups. The strong band at $1,586 \text{ cm}^{-1}$ is attributed to the O–H stretching mode in the central O–H–O system. A strong absorption bands at 1,097, 796, 729 and 606 cm^{-1} ; it is observed that the first two bands are assigned for symmetric stretching and in-plane vibration of Si–O groups; and last two bands are ascribed to the perpendicular stretching of Si–O groups [13]. The strong peaks at 549 and 454 cm^{-1} are corresponds to the deformation vibration of –OH inner hydroxyl groups of Al_2OH , Al–O–Si and Si–O–Si [14]. After modified MFA, a strong and broad peak at $1,006 \text{ cm}^{-1}$ corresponds to the Ti–O–Ti group [15] and a sharp absorption peak at $3,771 \text{ cm}^{-1}$ is ascribed to the O–H stretching of Ti–OH group [16]. This result confirms that the titanium dioxide group binds to the surface of FA.

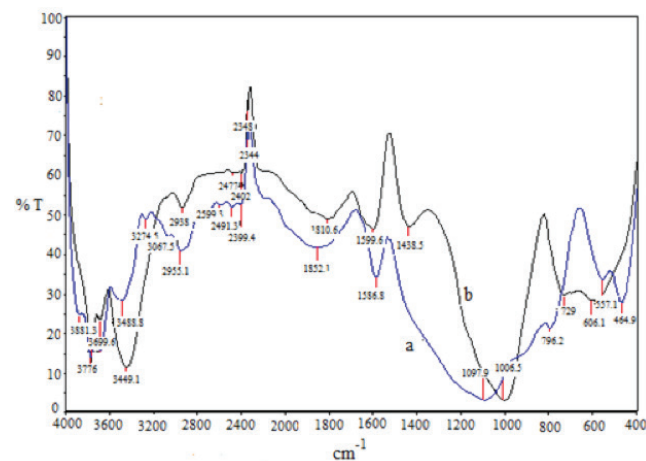


Fig. 1. FTIR analysis: (a) FA and (b) MFA.

3.1.2. SEM with EDX of FA and MFA

The morphology and surface texture of individual particles as well as elemental composition of a material can be obtained using SEM and EDX. Fig 2(a) shows the EDX spectra of FA, the inset being the SEM image of FA showing the presence of spherical particles of various sizes. It can be observed from image that these spheres exhibit several morphology and textures on the surface of these particles. The EDX spectra taken at different spot areas of the homogeneous regions (selected visually) of the SEM images of the specimen. Fig. 2(a) confirms the presence of O, Si, Al and Fe, with the concentration of 43.58, 30.47, 19.29 and 2.86 wt%, respectively, as the major constituents on the surface of FA.

Fig. 2(b) (inset) shows the SEM image of MFA composite particle where a non-uniform layer consisting of titanium deposited on the surface of FA particle. The comparison of EDX spectrum, Fig. 2(b), with that presented in Fig. 2(a) confirms the deposition of TiO_2 (22.7 wt%) on the surface of FA particles.

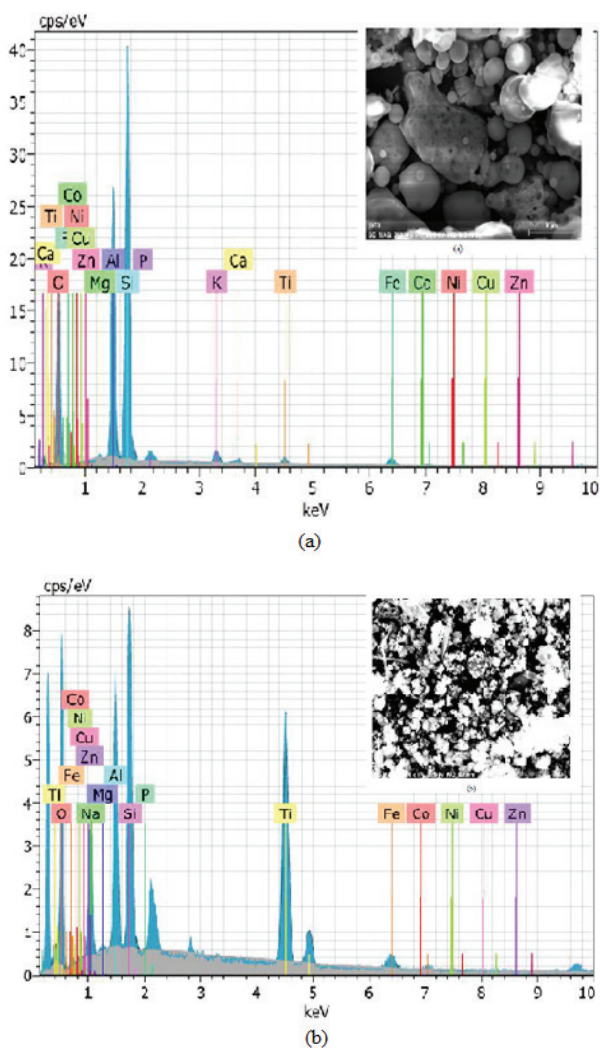


Fig. 2. SEM-EDX: (a) FA and (b) MFA.

3.1.3. X-ray diffraction

The XRD results of FA and MFA are shown in (Figs. 3(a) and (b)), respectively. Crystalline structure of MFA with the formation of limited components like monocline coesite (SiO_2), hematite syn (Fe_2O_3) is observed from Fig. 3(b). The XRD data show MFA is well embedded with TiO_2 showing the hump between $2\theta = 20^\circ$ and $2\theta = 30^\circ$. In Fig. 3(b), identified with higher values, a strong anatase peak at $2\theta = 25.38^\circ$ indicates dissolution of FA and new phase formation during hydrothermal process. It is about 73.7% crystalline in case of MFA.

3.2. Effect of operating variables

3.2.1. Effect of adsorbent dosage

The effect of adsorbent dosage on Zn(II) and Ni(II) ions removal was studied by varying the amount of adsorbent (2–14 g L^{-1} of MFA) keeping other parameters (pH 6, temperature 303 K, contact time 180 min, agitation speed 150 rpm) constant and is shown in Fig. 4. It can be observed from Fig. 4 that the adsorption capacity decreases from 0.203 to 0.046 mg g^{-1} for Ni(II) and 0.223 to 0.061 mg g^{-1} for Zn(II) with increase in

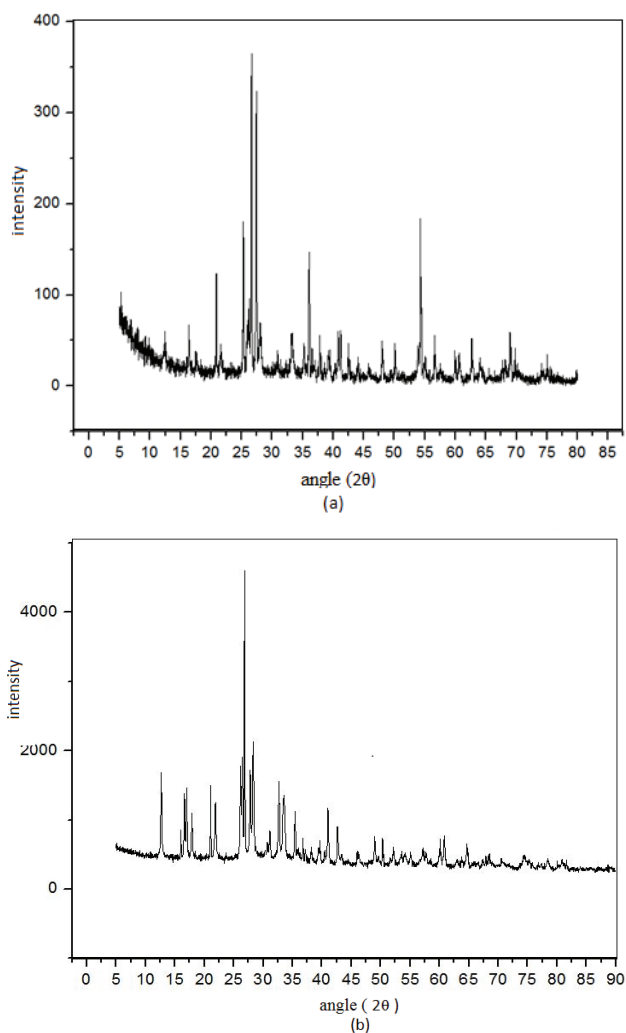


Fig. 3. XRD graph: (a) FA and (b) MFA.

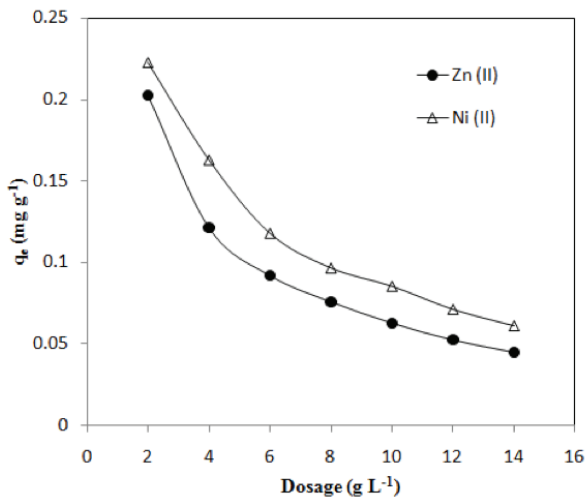


Fig. 4. Effect of adsorbent dosage: initial metal concentration, 10 mg L⁻¹; contact time, 180 min; pH, 6; 150 rpm.

dosage. In both the cases, the amount of metal ions adsorbed per unit weight of adsorbent (q_e) decreases with increase in MFA dosage. This is due to the fact that the solution metal ion concentration drops to a lower value at higher carbon dose and the system attains equilibrium at lower values of ' q_e ' indicating unsaturation of the adsorption sites [17].

3.2.2. Effect of time and initial concentration

The adsorption capacity is dependent on the initial metal ion concentration. The dependence of adsorption capacity of MFA on Zn(II) and Ni(II) ions removal is shown in Fig. 5. It can be observed from Fig. 5 that the increase in adsorption capacity with an increase in initial metal ion concentration may be due to increase in driving force due to concentration gradient developed between the bulk solution and surface of the adsorbent [18]. It can also be observed that adsorption process for both metal ions is rapid at initial stage and gradually reaches maximum removal at an equilibrium time of 180 min. This may be due to the fact that, at initial stage there are large numbers of active sites available for the removal of metal ions.

3.2.3. Effect of pH

The effect of pH on Zn(II) and Ni(II) ions removal was studied by varying pH from 4 to 8, keeping other parameters (concentration of metal ions 10 mg L⁻¹, adsorbent dosage 12 g L⁻¹ for Zn(II) and 10 mg L⁻¹ for Ni(II) ions, 150 rpm) constant and the results shown in Fig. 6. The effect of pH on Zn(II) removal can be explained considering the surface charge on the adsorbent material. At low pH, due to high positive charge density on the surface sites electrostatic repulsion between metal ion and H⁺ ion will be high resulting in lower removal efficiency. With increasing pH, electrostatic repulsion decreases due to reduction of positive charge density of proton on the sorption sites thus resulting in an enhancement of metal adsorption. Decrease in adsorption at higher pH (greater than 6) may be due to the formation of soluble hydroxyl complexes [19].

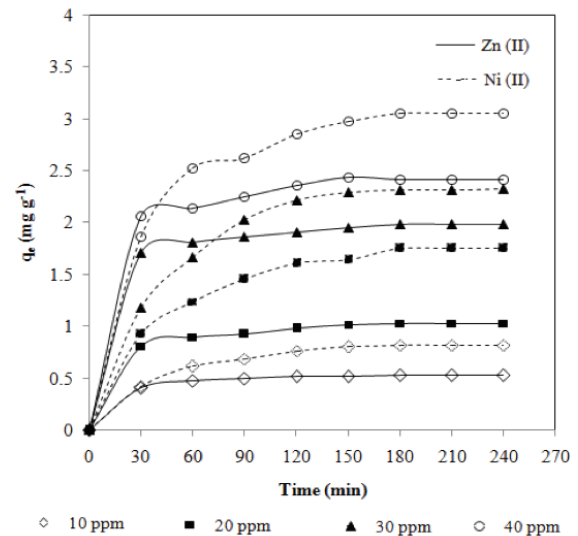


Fig. 5. Effect of initial metal ion concentration: pH, 6; 150 rpm; adsorbent dosage, 12 g L⁻¹ for Zn(II) and 10 g L⁻¹ for Ni(II) ions.

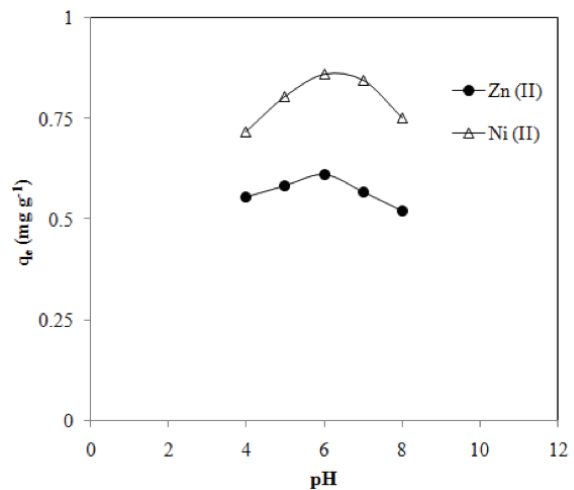


Fig. 6. Effect of pH: 150 rpm; adsorbent dosage, 12 g L⁻¹ for Zn(II) and 10 g L⁻¹ for Ni(II) ions.

In the case of Ni(II), there was an increase followed by decrease in adsorption capacity with initial pH varying from 4.0 to 8.0 and the maximum adsorption capacity was observed at pH 6.0. When the pH exceeds 6, the uptake decreases because Ni(II) ion starts to precipitate as Ni(OH)₂ at higher pH. Similar finding has been reported in the literature [20].

3.2.4. Effect of temperature

To study the thermodynamic properties of adsorption, experiments were carried out at different temperatures (303, 313 and 323 K) and results shown in Fig. 7. It can be observed from Fig. 7 that the adsorption capacity for Ni(II) and Zn(II) ions from 0.8225 to 0.7107 mg g⁻¹ and 0.5325 to 0.4997 mg g⁻¹, respectively, with increase in temperature. The adsorption

equilibrium data obtained for different temperatures were used to calculate the important thermodynamic properties such as standard Gibbs free energy (ΔG°), standard enthalpy change (ΔH°) and standard entropy change (ΔS°). The Gibbs free energy was determined using the following equation [21]:

$$\Delta G^\circ = -RT(\ln K_c) \quad (2)$$

This relationship can be used to determine constant value of K_c

$$K_c = \left[\frac{C_{Be}}{C_{Ae}} \right] \quad (3)$$

where C_{Ae} and C_{Be} are metal ion equilibrium concentration of solution and adsorbent (mg L^{-1}). The standard entropy and enthalpy can be determined by using Van 't Hoff equation

$$\ln K_c = \left[\frac{\Delta S^\circ}{R} - \frac{\Delta H^\circ}{RT} \right] \quad (4)$$

The standard entropy and enthalpy ΔS° and ΔH° can be determined by using the plot of $\ln K_c$ vs. $1/T$. The thermodynamic parameters for both metal ions are tabulated in Table 2.

The values of ΔG° ranges from -2.801 to -2.332 kJ mol^{-1} for Zn(II) and -2.133 to -0.874 kJ mol^{-1} for Ni(II) ions indicating that electrostatic attraction is the major mechanism responsible for the metal ion adsorption process. The negative value of ΔG° and ΔH° shows that the process is spontaneous and exothermic.

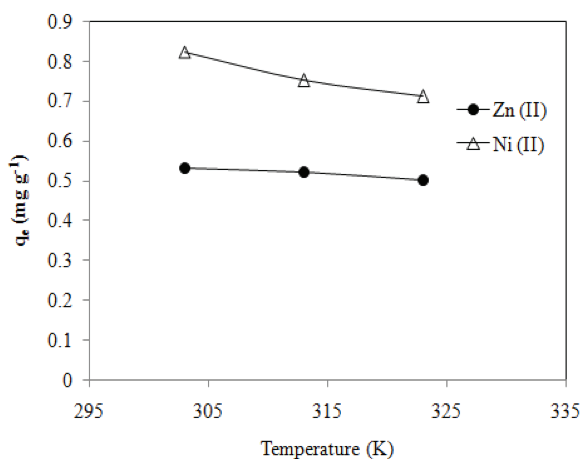


Fig. 7. Effect of temperature: initial metal concentration, 10 g L^{-1} ; contact time, 180 min; pH, 6; 150 rpm.

Table 2
Thermodynamic parameters for the adsorption of zinc on modified fly ash surface

Temperature (K)	Zn(II)			Ni(II)		
	ΔG° (kJ mol^{-1})	ΔS° (kJ mol^{-1})	ΔH° ($\text{J mol}^{-1} \text{K}^{-1}$)	ΔG° (kJ mol^{-1})	ΔS° (kJ mol^{-1})	ΔH° ($\text{J mol}^{-1} \text{K}^{-1}$)
303	-2.8019	-3.3003	-0.0238	-2.1331	-11.7920	-0.0514
313	-2.6457			-1.3172		
323	-2.3315			-0.8735		

3.3. Kinetics studies

The kinetics study indicates the rate of the solute adsorption and adsorbate residence time into the solid solution. The adsorption mechanism depends on the characteristics of adsorbent and its mass transfer process. The kinetics of Zn(II) and Ni(II) removal onto MFA are done by fitting the experimental data using pseudo-first-order and pseudo-second-order model.

3.3.1. Pseudo-first-order model

The linear form of this model is given as:

$$\log(q_e - q_t) = \log q_e - \frac{k_1}{2.303} t \quad (5)$$

where q_e (mg g^{-1}) denotes equilibrium concentration of ions in solution, q_t (mg g^{-1}) represents residual concentration and k_1 (min^{-1}) is first-order rate constant. The pseudo-first-order rate constant k_1 is determined from slope and intercept of plot $\log(q_e - q_t)$ vs. t . The straight line plots of $\log(q_e - q_t)$ vs. t were made for different initial metal concentrations to obtain the rate constants and equilibrium metal uptake (not shown).

It was concluded from the R^2 values (Table 3) through statistical analysis that the adsorption mechanism for both metal ions onto MFA does not follow the pseudo-first-order kinetic model.

3.3.2. Pseudo-second-order model

The pseudo-second-order model shows the rate of site occupied is proportional to square of unoccupied sites. The linear form of the equation is given as [22]:

$$\frac{t}{q_t} = \frac{1}{k_2 q_e^2} + \frac{1}{q_e} t \quad (6)$$

A linear plot of t/q_t vs. t for the pseudo-second-order model for the adsorption is shown in (Figs. 8(a) and (b)). The rate constants k_2 , R^2 and q_e values are reported in Table 3.

It can be observed from table that the R^2 values for pseudo-second-order model for both metal ions are higher and the calculated q_e values are closer to the experimental q_e values confirming that it fits well.

3.4. Adsorption isotherms

Equilibrium relationships between adsorbent and adsorbate are explained using Langmuir, Freundlich, Temkin and Dubinin–Radushkevich isotherm models.

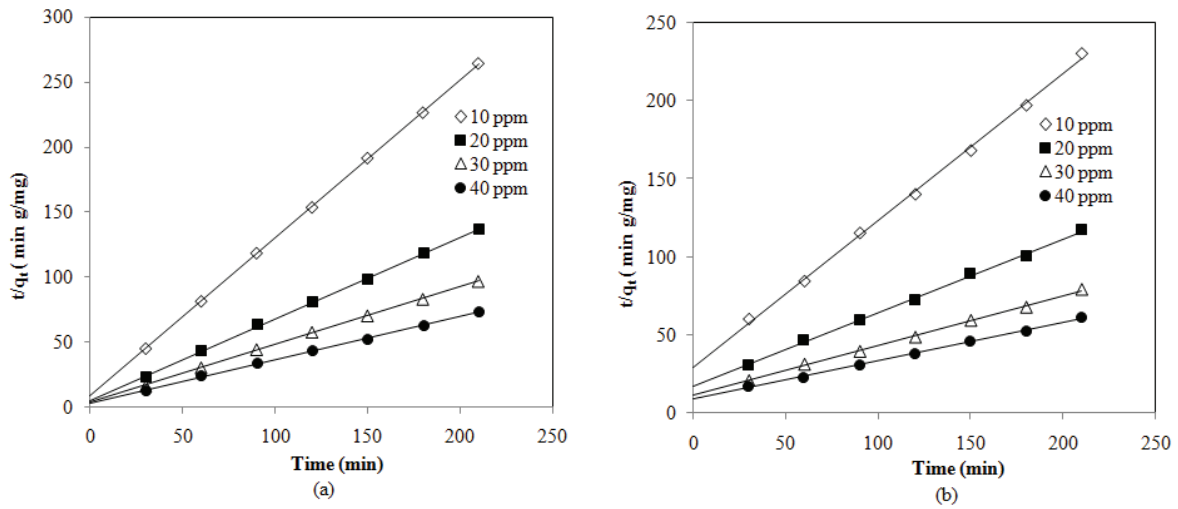


Fig. 8. Pseudo-second-order models: pH, 6; 150 rpm. (a) Zn(II) and (b) Ni(II) ions.

Table 3
Kinetic parameters for Zn(II) and Ni(II) adsorption on MFA

Metal ions	Concentrations (ppm)	$(q_e)_{exp}$ (mg g ⁻¹)	Pseudo-first-order			Pseudo-second-order		
			k_1 (1 min ⁻¹)	q_e (mg g ⁻¹)	R^2	k_2 (g mg ⁻¹ min ⁻¹)	q_e (mg g ⁻¹)	R^2
Zn(II)	10	0.7957	0.1082	0.9540	0.815	0.1776	0.8133	0.9998
	20	1.524	0.0506	0.9782	0.528	0.0792	1.5949	0.9993
	30	2.169	0.0529	1.1773	0.797	0.0618	2.2421	0.9991
	40	2.8623	0.0506	1.9783	0.712	0.04547	2.9851	0.9992
Ni(II)	10	0.9998	0.0552	0.9636	0.786	0.0373	1.0351	0.998
	20	1.920	0.0368	1.1864	0.874	0.0143	2.083	0.995
	30	2.7867	0.0345	1.4696	0.596	0.0137	2.8167	0.997
	40	3.6867	0.0299	1.6144	0.751	0.0094	3.798	0.998

3.4.1. Langmuir isotherm

The monolayer deposition on adsorbent is indicated using Langmuir isotherm. The Langmuir equation is given as follows [23]:

$$q_e = \left[\frac{X_m b C_e}{1 + b C_e} \right] \tag{7}$$

where 'b' is the binding constant, C_e is the equilibrium concentration of metal ion in the solution (mg L⁻¹), q_e is amount of the metal ion adsorbed at equilibrium (mg g⁻¹) and X_m refers the maximum adsorption capacity, evaluated by plotting C_e/q_e against C_e .

The estimated b , X_m and R^2 for both metal ions are tabulated in Table 4(a). It can be noticed that the Langmuir isotherm model does not match well with the experimental observation.

3.4.2. Freundlich isotherm

The relationship between adsorption intensity of adsorbent towards adsorbate is given by Freundlich isotherm. This isotherm describes reversible adsorption and not restricted to monolayer formation. The equation is represented as [24]:

$$q_e = K_f C_e^{1/n} \tag{8}$$

where n and K_f are the constant describing adsorption intensity and adsorption capacity. The linear form of this equation can be written as follows:

$$\ln q_e = \ln K_f + \frac{1}{n} \ln C_e \tag{9}$$

The n , K_f and R^2 values are calculated from the plot $\ln q_e$ vs. $\ln C_e$ (Figs. 9(a) and (b)) and tabulated in Table 4(a), for both metal ions. The estimated R^2 values of Freundlich isotherm indicates that the experimental data fits well with predicted value for this model.

3.4.3. Temkin isotherm

Temkin and Pyzhev [25] considered adsorbent/adsorbate interactions and represented the equation as:

$$q_e = B \ln A + B \ln C_e \tag{10}$$

where $B = RT/b$, B , A and T are constants. A plot of q_e vs. $\ln C_e$ helps to find out A and B . The estimated A , B and R^2 are given

Table 4(a)
Langmuir and Freundlich model parameters for Zn(II) and Ni(II) ions

Metal ions	Concentrations (ppm)	Langmuir parameters			Freundlich parameters		
		q_{\max} (mg g ⁻¹)	b (L mg ⁻¹)	R^2	K_F (L g ⁻¹)	N	R^2
Zn(II)	10	4.397	2.041	0.891	0.761	11.873	0.993
	20	3.278	0.926	0.994	1.603	9.638	0.999
	30	1.426	0.422	0.794	2.832	5.208	0.995
	40	0.952	0.2124	0.889	3.877	3.714	0.999
Ni(II)	10	6.226	5.042	0.778	0.901	9.009	0.957
	20	3.201	4.902	0.897	1.982	7.042	0.998
	30	1.797	4.028	0.988	3.232	6.369	0.971
	40	0.939	2.632	0.8195	4.797	5.181	0.963

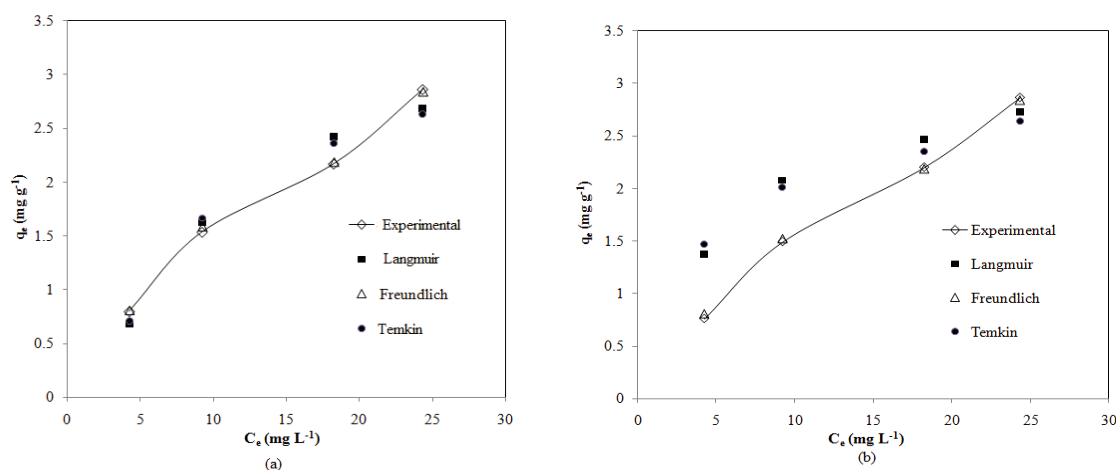


Fig. 9. Comparison of isotherm model prediction with the experimental observations: pH, 6; contact time, 180 min; 150 rpm. (a) Zn(II) and (b) Ni(II) ions.

Table 4(b)
Temkin parameters and Dubinin–Radushkevich (D–R) parameters for Zn(II) and Ni(II) ions

Metal ions	Concentrations (ppm)	Temkin parameters			(D–R) parameters		
		A (L g ⁻¹)	B	R^2	q_m (mg g ⁻¹)	K	R^2
Zn(II)	10	1.685	-0.05	0.993	0.944	0.00000003	0.472
	20	2.7376	-0.144	0.899	1.434	0.00000005	0.727
	30	3.0821	-0.402	0.9774	1.885	0.00000009	0.574
	40	5.1153	-0.496	0.7173	2.577	0.00000008	0.692
Ni(II)	10	0.899	-0.088	0.736	0.892	0.000000001	0.539
	20	1.977	-0.249	0.937	1.608	0.00000003	0.703
	30	3.164	-0.408	0.977	2.370	0.00000003	0.839
	40	4.555	-0.646	0.866	3.025	0.00000008	0.457

in Table 4(b) for both metal ions and it was found that model does not fit with experimental observations.

3.4.4. Dubinin–Radushkevich model

The Dubinin–Radushkevich (D–R) isotherm does not consider constant adsorption potential rate and homogeneous surface and expressed as [26]:

$$q_e = q_m \exp(-K_e^2) \quad (11)$$

The linear form of D–R is given as:

$$\ln q_e = \ln q_m - K_e^2 \quad (12)$$

where q_e is the amount of the metal ion adsorbed at equilibrium, K is a constant related to the mean free energy

Table 5
Comparison of adsorption capacity of various adsorbents with MFA

Adsorbent	Adsorption capacity (mg g ⁻¹)		References
	Zn(II)	Ni(II)	
Commercial activated carbon		1.49	[27]
Hazelnut husk activated carbon		5.76	[28]
Peanut hull		1.58	[29]
Chitosan		2.4	[30]
Palm shell activated carbon		0.13	[31]
Black locust	4.02		[32]
Sugar beet pulp	0.176		[33]
Fly ash	0.75		[34]
Chestnut shell	2.4		[35]
Carbon slurry	2.5	1.03	[35]
Wheat straw	3.25	2.5	[36]
Coir fibre	1.83	2.51	[37]
MFA	4.397	6.226	Present study

Table 6
Error analysis for Zn(II) adsorption on MFA

Isotherms	Sum-of-squared errors	HYBRID	Marquardt's percent standard deviation	Average relative error	Sum of absolute error
Zn(II)					
pH 4					
Langmuir	0.241	3.631	12.185	9.839	0.813
Freundlich	0.038	1.114	6.094	4.408	0.308
DR	7.060	21.265	30.886	16.134	2.939
Tempkin	0.180	0.860	15.480	11.848	0.780
pH 5					
Langmuir	0.100	9.346	8.554	7.009	0.521
Freundlich	0.029	2.603	4.471	3.474	0.277
DR	2.346	17.237	23.248	12.928	1.815
Tempkin	0.402	5.585	22.477	17.227	1.093
pH 6					
Langmuir	0.115	1.518	11.901	9.547	0.632
Freundlich	0.003	0.839	2.075	1.396	0.093
DR	0.842	18.874	18.607	14.155	1.602
Tempkin	0.115	0.789	10.793	9.243	0.645
pH 7					
Langmuir	0.149	1.122	11.433	9.088	0.662
Freundlich	0.028	0.498	5.053	3.973	0.299
DR	0.600	13.301	15.866	9.975	1.120
Tempkin	0.150	0.438	11.006	9.343	0.694
pH 8					
Langmuir	0.154	9.012	12.659	9.219	0.623
Freundlich	0.091	5.164	8.025	6.833	0.518
DR	0.673	10.222	18.044	15.102	1.553
Tempkin	0.138	4.921	17.273	11.132	0.602

of adsorption, q_m is the theoretical saturation capacity. The estimated K , q_m and R^2 tabulated in Table 4(b) for both heavy metal ions reveals that the model does not give a good fit.

The maximum adsorption capacity of Zn(II) and Ni(II) ions evaluated is 4.397 and 6.226 mg g⁻¹, respectively. Table 5 shows comparison of adsorption capacity of various adsorbents with MFA for Zn(II) and Ni(II) ions [27–37].

3.5. Error estimation

To minimize the error distribution between the experimental equilibrium data and isotherms, error functions such as the sum-of-squared errors, the hybrid fractional error function (HYBRID), the Marquardt's percent standard deviation, the average relative error and the sum of absolute error [38,39] were used. The error deviations between experimental and predicted equilibrium adsorption data are tabulated in Tables 6 and 7. From tables, the error functions corresponding to the minimized deviations suggested that the Freundlich isotherm fitted the adsorption data the best for both the metal ions.

Table 7
Error analysis for Ni(II) adsorption on MFA

Isotherms	Sum-of-squared errors	HYBRID	Marquardt's percent standard deviation	Average relative error	Sum of absolute error
Ni(II)					
pH 4					
Langmuir	0.388	15.583	15.784	11.687	0.947
Freundlich	0.012	3.214	4.038	2.622	0.169
DR	8.890	41.959	41.580	31.469	4.864
Tempkin	2.389	54.159	48.257	40.619	2.802
pH 5					
Langmuir	2.163	56.079	50.099	42.059	2.824
Freundlich	0.021	5.837	7.312	4.832	0.252
DR	4.922	41.146	36.754	30.859	4.193
Tempkin	1.884	43.706	42.567	32.779	2.312
pH 6					
Langmuir	0.797	23.651	28.555	17.738	1.181
Freundlich	0.022	6.466	6.495	4.849	0.272
DR	19.821	39.127	41.238	29.345	6.094
Tempkin	4.939	62.160	55.969	46.620	3.811
pH 7					
Langmuir	0.991	28.432	26.739	21.324	1.677
Freundlich	0.007	3.794	4.928	2.905	0.143
DR	6.313	22.579	31.622	20.550	3.259
Tempkin	1.270	23.603	26.463	20.403	1.794
pH 8					
Langmuir	2.231	55.195	48.363	41.396	2.813
Freundlich	0.140	12.691	13.016	9.518	0.588
DR	7.921	43.910	40.479	32.933	4.849
Tempkin	1.602	50.263	45.588	37.697	2.393

4. Conclusions

Adsorption experiments were carried out in a batch mode to remove Zn(II) and Ni(II) ion from synthetic wastewater using hydrothermally MFA. The characterisation of the FA and MFA using XRD, FTIR and SEM with EDX was done. The effect of various parameters on adsorption was studied and adsorption equilibrium attained at 180 min with optimum pH of 6 for both the metal ions. The kinetic study reveals that the adsorption follows pseudo-second-order model. The isotherm models like Langmuir, Freundlich, Temkin and Dubinin–Radushkevich isotherm models were used to describe the adsorption and it was found that the experimental data fitted well with predicted value in case of Freundlich isotherm. The adsorption capacity obtained were 4.397 and 6.226 mg g⁻¹ for Zn(II) and Ni(II) ions, respectively. The thermodynamic parameters evaluated indicate that the process is spontaneous and exothermic for both metal ions.

Symbols

A	— Temkin constants relating to sorption potential, L g ⁻¹
b	— Langmuir constant representing adsorption intensity, L mg ⁻¹
B	— Temkin constants relating to heat of adsorption
C_0	— Initial concentration of metal ion in solution, mg L ⁻¹
C_e	— Equilibrium concentration of metal ion in solution, mg L ⁻¹
k_1	— Pseudo-first-order rate constant, min ⁻¹
k_2	— Pseudo-second-order rate constant, g mg ⁻¹ min ⁻¹
m	— Mass of the adsorbent, g
n	— Adsorption intensity, g L ⁻¹
q_e	— Adsorption capacity at equilibrium, mg g ⁻¹
q_m	— Theoretical saturation capacity, mg g ⁻¹
q_t	— Adsorption capacity at any time t , mg g ⁻¹
R^2	— Correlation coefficient
t	— Contact time, min
T	— Temperature, K
V	— Volume of adsorbate solution, L
X_m	— Monomolecular adsorption capacity, mg g ⁻¹

Greek

ΔG°	— Standard Gibbs free energy change
ΔH°	— Standard enthalpy change
ΔS°	— Standard entropy change

References

- [1] B. Geng, Z. Jin, T. Li, X. Qi, Preparation of chitosan-stabilized Fe⁰ nanoparticles for removal of hexavalent chromium in water, *Sci. Total Environ.*, 407 (2009) 4994–5000.
- [2] R.M. Nthumbi, J.C. Ngila, B. Moodley, A. Kindness, L. Petrik, Application of chitosan/polyacrylamide nanofibres for removal of chromate and phosphate in water, *Phys. Chem. Earth*, 50–52 (2012) 243–251.
- [3] S.P. Dubey, K. Gopal, Adsorption of chromium(VI) on low cost adsorbents derived from agricultural waste material: a comparative study, *J. Hazard. Mater.*, 145 (2007) 465–470.
- [4] M.M. Areco, S. Hanela, J. Duran, M.S. Afonso, Biosorption of Cu(II), Zn(II), Cd(II) and Pb(II) by dead biomasses of green alga *Ulva lactuca* and the development of a sustainable matrix for adsorption implementation, *J. Hazard. Mater.*, 213–214 (2012) 123–132.
- [5] N. Caliskan, A.R. Kul, S. Alkan, E.G. Sogut, I. Alacabey, Adsorption of zinc(II) on diatomite and manganese-oxide-modified diatomite: a kinetic and equilibrium study, *J. Hazard. Mater.*, 193 (2011) 27–36.
- [6] A.B. Pérez-Marín, A. Ballester, F. González, M.L. Blázquez, J.A. Muñoz, J. Sáez, V.M. Zapata, Study of cadmium, zinc and lead biosorption by orange wastes using the subsequent addition method, *Bioresour. Technol.*, 99 (2008) 8101–8106.
- [7] M. Visa, A. Duta, Methyl-orange and cadmium simultaneous removal using fly ash and photo-fenton systems, *J. Hazard. Mater.*, 244 (2013) 773–779.
- [8] M. Visa, A.-M. Chelaru, Hydrothermally modified fly ash for heavy metals and dyes removal in advanced wastewater treatment, *Appl. Surf. Sci.*, 303 (2014) 14–22.
- [9] A. Adamczuk, D. Kolodynska, Equilibrium, thermodynamic and kinetic studies on removal of chromium, copper, zinc and arsenic from aqueous solutions onto fly ash coated by chitosan, *Chem. Eng. J.*, 274 (2015) 200–212.
- [10] T.C. Hsu, C.C. Yu, C.M. Yeh, Adsorption of Cu²⁺ from water using raw and modified coal fly ashes, *Fuel*, 87 (2008) 1355–1359.
- [11] A.D. Papandreou, C.J. Stournaras, D. Panias, I. Paspaliaris, Adsorption of Pb(II), Zn(II) and Cr(III) on coal fly ash porous pellets, *Miner. Eng.*, 24 (2011) 1495–1501.
- [12] M. Visa, L. Isac, A. Duta, New fly ash TiO₂ composite for the sustainable treatment of wastewater with complex pollutants load, *Appl. Surf. Sci.*, 339 (2015) 62–68.
- [13] T. Bakharev, Geopolymeric materials prepared using Class F fly ash and elevated temperature curing, *Cem. Concr. Res.*, 35 (2005) 1224–1232.
- [14] S. Meenakshi, K. Pandian, Simultaneous voltammetry detection of dopamine and uric acid in pharmaceutical products and urine samples using ferrocene carboxylic acid primed nanoclay modified glassy carbon electrode, *J. Electrochem. Soc.*, 163 (2016) B543–B555.
- [15] Z. Liu, Z. Jian, J. Fang, X. Xu, X. Zhu, S. Wu, Low-temperature reverse microemulsion synthesis, characterization, and photocatalytic performance of nanocrystalline titanium dioxide, *Int. J. Photoenergy*, 2012 (2012) 1–8.
- [16] F. Hirose, K. Kuribayashi, T. Suzuki, Y. Narita, Y. Kimura, M. Niwano, UV treatment effect on TiO₂ electrodes in dye-sensitized solar cells with N719 sensitizer investigated by infrared absorption spectroscopy, *Electrochem. Solid-State Lett.*, 11 (2008) A109–A111.
- [17] T.K. Naiya, P. Chowdhury, A.K. Bhattacharya, S. Kumar Das, Saw dust and neem bark as low-cost natural biosorbent for adsorptive removal of Zn(II) and Cd(II) ions from aqueous solutions, *Chem. Eng. J.*, 148 (2009) 68–79.
- [18] Z. Khademi, B. Ramavandi, M. Taghi Ghaneian, The behaviors and characteristics of a mesoporous activated carbon prepared from *Tamarix hispida* for Zn(II) adsorption from wastewater, *J. Environ. Chem. Eng.*, 3 (2015) 2057–2067.
- [19] R.J.E. Martins, R. Pardo, R.A.R. Boaventura, Cadmium(II) and zinc(II) adsorption by the aquatic moss *Fontinalis antipyretica*: effect of temperature, pH and water hardness, *Water Res.*, 38 (2004) 693–699.
- [20] K. Chithra, Shweta Lakshmi and Abhishek Jain, Carica papaya seed as a biosorbent for removal of Cr (VI) and Ni (II) ions from aqueous solution, *Int. J. Chem. React. Eng.*, 12 (2014) 1–12.
- [21] Y. Liu, Y.-J. Liu, Biosorption isotherms, kinetics and thermodynamics, *Sep. Purif. Technol.*, 61 (2008) 229–242.
- [22] M. Danish, M. Rokiah Hashim, N.M. Ibrahim, M. Rafatullah, O. Sulaiman, T. Ahmad, M. Shamsuzzoha, A. Ahmad, Sorption of copper(II) and nickel(II) ions from aqueous solutions using calcium oxide activated carbon: equilibrium, kinetic, and thermodynamic studies, *J. Chem. Eng.*, 56 (2011) 3607–3619.
- [23] I. Langmuir, The adsorption of gases on plane surfaces of glass, mica and platinum, *J. Am. Chem. Soc.*, 40 (1918) 1361–1403.
- [24] H.M.F. Freundlich, Over the adsorption in solution, *J. Phys. Chem.*, 57 (1906) 385–471.
- [25] M.J. Temkin and V. Pyzhev, Kinetics of ammonia synthesis on promoted iron catalysts, *Acta. Physicochim.*, 12 (1940) 217–222.

- [26] M.M. Dubinin, The potential theory of adsorption of gases and vapors for adsorbents with energetically non-uniform surface, *Chem. Rev.*, 60 (1960) 235–241.
- [27] K. Kadirvelu, K. Thamaraiselvi, C. Namasivayam, Adsorption of nickel(II) from aqueous solution onto activated carbon prepared from coirpith, *Sep. Purif. Technol.*, 24 (2001) 497–505.
- [28] E. Demirbas, M. Kobya, S. Oncel, S. Sencan, Removal of Ni(II) from aqueous solution by adsorption onto hazelnut shell activated carbon: equilibrium studies, *Bioresour. Technol.*, 84 (2002) 291–293.
- [29] K. Periasamy, C. Namasivayam, Removal of nickel(II) from aqueous solution wastewater using an agricultural waste: peanut hulls, *Waste Manage.*, 15 (1995) 63–68.
- [30] R.S. Singh, V.K. Singh, P.N. Tiwari, U.N. Singh, Y.C. Sharma, An economic removal of Ni(II) from aqueous solutions using an indigenous adsorbent, *Open Environ. Eng. J.*, 2 (2009) 30–36.
- [31] Y.B. Onundi, A.A. Mamun, M.F. Al Khatib, Y.M. Ahmed, Adsorption of copper, nickel and lead ions from synthetic semiconductor industrial wastewater by palm shell activated carbon, *Int. J. Environ. Sci. Technol.*, 7 (2010) 751–758.
- [32] M. Sciban, M. Klasnja, B. Skrbic, Modified hardwood saw dust as adsorbent of heavy metal ions from water, *Wood Sci. Technol.*, 40 (2006) 217–227.
- [33] E. Pehlivan, S. Cetin, B.H. Yanik, Equilibrium studies for the sorption of zinc and copper from aqueous solutions using sugar beet pulp and fly ash, *J. Hazard. Mater.*, 135 (2006) 193–199.
- [34] C.H. Weng, C.P. Huang, Adsorption characteristics of Zn(II) from dilute aqueous solution by fly ash, *Colloids Surf., A*, 247 (2004) 137–143.
- [35] G. Vázquez, M. Calvo, M. Sonia Freire, J. González-Alvarez, G. Antorrena, Chestnut shell as heavy metal adsorbent: optimization study of lead, copper and zinc cations removal, *J. Hazard. Mater.*, 172 (2009) 1402–1414.
- [36] M. Gorgievski, D. Bozic, V. Stankovic, N. Strbac, S. Serbula, Kinetics, equilibrium and mechanism of Cu²⁺, Ni²⁺ and Zn²⁺ ions biosorption using wheat straw, *Ecol. Eng.*, 58 (2013) 113–122.
- [37] S.R. Shukla, R.S. Pai, A.D. Shendarkar, Adsorption of Ni(II), Zn(II) and Fe(II) on modified coir fibre, *Sep. Purif. Technol.*, 47 (2006) 141–147.
- [38] M. Hadi, M.R. Samarghandi, G. McKay, Equilibrium two-parameter isotherms of acid dyes sorption by activated carbons: study of residual errors, *Chem. Eng. J.*, 160 (2010) 408–416.
- [39] L.S. Chan, W.H. Cheung, S.J. Allen, G. McKay, Error analysis of adsorption isotherm models for acid dyes onto bamboo derived activated carbon, *Chin. J. Chem. Eng.*, 20 (2012) 535–542.